

1 **APPLICATION OF BIAS CORRECTION METHODS**

2 **TO IMPROVE THE ACCURACY OF QUANTITATIVE RADAR**

3 **RAINFALL IN KOREA**

5 Jae-Kyoung Lee¹, Ji-Hyeon Kim², and Mi-Kyung Suk²

6

7 1 Innovation Center for Engineering Education, Daejin University, Pocheon-si, Gyeonggi-do,
8 Korea

9 2 Weather Radar Center, Korea Meteorological Administration, Seoul, Korea

10

11

12 17 March 2015

13

14

15

16

17

18

19

20 Corresponding Author: Jae-Kyoung Lee, Innovation Center for Engineering Education,
21 Daejin University, Hoguk-ro 1007, Pocheon-si, Gyeonggi-do, 487-711, Korea
22 E-mail : myroom1@daejin.ac.kr

1

Abstract

2 There are many potential sources of bias in the radar rainfall estimation process. This
3 study classified the biases from the rainfall estimation process into the reflectivity
4 measurement bias and QPE model bias and also conducted the bias correction methods to
5 improve the accuracy of the Radar-AWS Rainrate (RAR) calculation system operated by the
6 Korea Meteorological Administration (KMA). For the Z-bias correction, this study utilized
7 the bias correction algorithm for the reflectivity. The concept of this algorithm is that the
8 reflectivity of target single-pol radars is corrected based on the reference dual-pol radar
9 corrected in the hardware and software bias. This study, and then, dealt with two post-process
10 methods, the Mean Field Bias Correction (MFBC) method and the Local Gauge Correction
11 method (LGC), to correct rainfall-bias. The Z-bias and rainfall-bias correction methods were
12 applied to the RAR system. The accuracy of the RAR system was improved after correcting
13 Z-bias. For rainfall types, although the accuracy of Changma front and local torrential cases
14 was slightly improved without the Z-bias correction, especially, the accuracy of typhoon cases
15 got worse than existing results. As a result of the rainfall-bias correction, the accuracy of the
16 RAR system performed Z-bias_LGC was especially superior to the MFBC method because
17 the different rainfall biases were applied to each grid rainfall amount in the LGC method. For
18 rainfall types, Results of the Z-bias_LGC showed that rainfall estimates for all types was
19 more accurate than only the Z-bias and, especially, outcomes in typhoon cases was vastly
20 superior to the others.

1 **Keywords:** Bias correction, Radar-AWS Rainrate calculation system, Local Gauge

2 Correction, Radar rainfall estimates

3

4

5

6

7

8

9

10

11

12

13

14

15

16

1 1. INTRODUCTION

2 Weather radars can provide rainfall estimates over the Korean Peninsula and near seas
3 with high spatial (minimum 0.125 km) and temporal resolutions (2.5 minutes), especially, and
4 play an important role in predicting and monitoring severe weather conditions. However,
5 several sources of bias are involved in the process of calculating quantitative radar-based
6 rainfall estimates. It is well acknowledged that radar data are affected by both systematic bias
7 (due to reflectivity measurements (included in hardware errors, signal processing, and quality
8 controls), parameter estimation of the Z - R relationship, and quantitative precipitation
9 estimation model structures) and random error (Huff, 1970; Woodely *et al.*, 1957, Wilson and
10 Brandes, 1979; Austin, 1987; Campos and Zawadzki, 2000; Krajewski and Smith, 2002)
11 because one of major reasons is that weather radars indirectly measure rainfall amounts using
12 the relations between measured radar variables and rainfall such as Z - R , Z_{DR} - R , and K_{DP} - R .
13 Related to systematic bias, a considerable number of studies have been conducted to correct
14 the reflectivity measurement bias which includes temporal and spatial sampling bias, ground
15 and sea clutter, beam-blockage and attenuation, electrical calibration, and quantification of
16 reflectivity bias (Chumchean *et al.*, 2006). Jordan *et al.* (2000) evaluated the errors which
17 arise in radar estimates of rainfall as a result of temporal sampling, spatial averaging,
18 measuring the field at some distance above the ground, and recording the reflectivity data
19 with a limited radiometric resolution. Germann *et al.* (2006) modified the ground clutter
20 algorithm and reduced the amount of residual non-meteorological signals in a mountainous
21 region, the Alps, to improve the precipitation estimation. Villarini and Krajewski (2008)
22 investigated the spatial sampling errors in radar observations which affect the sensitivity of

1 the models and determined that these errors were related to the approximation of an areal
2 estimate by a using a point measurement. Similarly, converting a measured reflectivity to
3 rainfall amount using artificial relationships or models is one of the major sources of bias. To
4 overcome these limitations, gauge adjustment methods were applied to correct misestimated
5 precipitation in numerous existing studies. Sinclair and Pegram (2005) described a merging
6 technique and presented an application of it to a simulated rainfall field. The proposed
7 merging technique based on Conditional Merging (CM) (Ehret, 2002) made use of a Kriging
8 method to reduce the bias while retaining spatial detail from the radar but keeping the spatial
9 variability observed by the radar. Morin and Gagella (2007) compared three radar-gauge
10 adjustment methods, a one-coefficient bulk adjustment, a Weighted Regression (WR), and a
11 Weighted Multiple Regression (WMR), for the radar-based quantitative precipitation
12 estimation over Mediterranean and dry climate regimes. They concluded the WR and WMR
13 adjustment methods were useful for calculating rain depth estimates, with some limitations.
14 Goudenhoofdt and Delobbe (2009) dealt with several radar-gauge merging methods
15 considering the gauge network densities and compared their precipitation estimates accuracy.
16 The analysis revealed that the simple methods reduced relatively the bias of radar estimation
17 and the geostatistical merging methods resulted in the better performance reflecting the gauge
18 network densities.

19 In a series of procedures which estimate the quantitative rainfalls derived from radar
20 information, the present paper focuses on correcting the measurement bias and bias in the
21 QPE model. The measurement bias is defined as the only reflectivity measurement bias
22 (hereafter Z-bias) which occurred while using weather radar hardware systems to detect

1 precipitation. The bias in the QPE model (hereafter QPE mode bias) is defined as the
2 estimated rainfall-bias which included the bias due to the parameters of the Z - R relationship,
3 the parameters of the QPE model, and the QPE model structure. Section 2 describes the
4 correction methods of the Z -bias and rainfall-bias and the QPE model used in this paper.
5 Section 3 gives results for rainfall estimations using the correction methods and describes the
6 effect of the Z -bias and rainfall-bias correction methods. Finally, Section 4 summarizes the
7 results and provides some concluding remarks.

8

9 **2. DATA AND METHODOLOGY**

10 **2.1 Radar Dataset and Rainfall Cases**

11 In this study, the performance of the bias correction methods has been evaluated by
12 comparing the observed rainfall data from rain gauges operated by the KMA (Korea
13 Meteorological Administration). Observed rainfall data were collected from 642 ground rain
14 gauges (called AWS, Automatic Weather Station) (321 rain gauges for the calibration and 321
15 rain gauges for the validation, respectively) located in the Korean Peninsula. The Bislsan S-
16 band dual-polarimetric radar which was installed and operated by the Ministry of Land,
17 Infrastructure and Transport (MLIT) beginning in 2009 was selected for the absolute
18 reference radar to estimate Z -bias (described in Section 2.2). Horizontal and vertical
19 reflectivity (Z_H and Z_V), differential reflectivity (Z_{DR}), differential phase (Φ_{DP}), specific
20 differential phase (K_{DP}), correlation coefficient (ρ_{HV}), and spectrum width (SW) are estimated
21 with a gate size of 0.125 km. The scan strategy has 6 elevation angles with a 2.5 minute

1 update cycle. The Accuracy of reference radar shows more than 80 % on average in
2 quantitative and qualitative test (You et al., 2014; Jeong et al., 2014; Kim et al., 2015). The
3 target radars which required Z-bias correction were 11 single-polarimetric radars
4 (Baegnyeondo, Kwanaksan, Oseonsan, Jindo, Gosan, Seongsan, Gudeoksan, Myeonbongsan,
5 Gangneung, Gwnagdeoksan, Incheon) with a scan range of the maximum 200 km (C-band)
6 and 240 km (S-band) and a gate size of 0.250 km operated by the KMA in Figure 1. Table
7 1(a) shows the radars and rain-gauges used for estimating Z-bias and data period and Table
8 1(b) shows 18 rainfall cases in the summer season used for the verification of the Z- and
9 rainfall-bias correction methods.

10

11 [Figure 1. Location of 11 single-polarization radars and the Bislsan S-band dual-polarization
12 radar and their observation ranges]

13 [Table 1. Summary of the Radars and Rainfall Cases]

14

15 **2.2 Quantitative Precipitation Estimation Model**

16 This paper has utilized the Radar-AWS Rainrate (RAR) calculation system (Hereafter
17 called the RAR system) for the QPE model. The RAR system which was developed by KMA
18 in 2006 is operated on site, based on 11 single-polarimetric radars. The RAR system produces
19 the merged rainfall field for the Korean Peninsula through a series of steps (production of the
20 radar reflectivity field, calculation of AWS rainfalls, derivation of the Z-R relationship, etc.)

1 (refer to Figure 2).

2 The RAR system estimates parameters of the Z-R relationship in real-time for real-time
3 rainfall estimates (Weather Radar Center, 2011). The RAR system utilizes 10-minute
4 reflectivity and AWS rainfall in the Window Probability Matching Method (WPMM)
5 (Rosenfeld *et al.*, 1993) to estimate rainfalls in each radar site and merged rainfalls of radar
6 sites for producing composite rainfall fields. Used reflectivity which are quality controlled
7 (removal of non-meteorological echoes) are averaged on 3 x 3 pixels with a certain AWS as
8 the center are used. The WPMM method reproduces the probability density functions (pdfs)
9 of ground rainfall from AWSs and radar reflectivity and determines the Z-R relationship
10 using these pdfs (refer to Equation (1) and (2)) (Rosenfeld *et al.*, 1993).

11

12
$$\int_0^{\infty} f(Z_e) P_c(Z_e) dZ_e = \int_0^{\infty} R P_c(R) dR \quad (1)$$

13
$$P_c(R) = P(R|R > R_T), \quad P_c(Z_e) = P(Z_e|Z_e > Z_{eT}) \quad (2)$$

14

15 Where Z_e is radar reflectivity (dBZ), $P_c()$ is the conditional probability function, R is rainfall
16 (mm/hr), and T is threshold. The conditional probability functions in Equation (1) are derived
17 from Equation (2) and thresholds of rainfall and radar reflectivity are 0.1 mm hr⁻¹ and 10 dBZ.
18 Parameters of the Z-R relationship have been estimated using radar reflectivity and AWS
19 rainfalls from 1 hour ago with the least square fit of power law. The number of radar
20 reflectivity and AWS rainfalls over a certain threshold are required to estimate parameters
21 accurately. If there is not enough data, estimated rainfalls from that Z-R relationship are

1 inaccurate. To overcome this limitation, if the number of available AWSs is more than 30%
2 of those available in each radar site, the parameters of the Z-R relationship can be estimated.
3 If less than 30%, $Z=200R^{1.6}$ (Marshall and Palmer, 1948) is applied for rainfall estimates
4 (Korea Meteorological Administration, 2012b).

5 Secondly, the composite rainfall field for the whole country may be produced using each
6 radar rainfall estimate. However, appropriate merging methods (the maximum value, average
7 value, minimum value, distance weighting methods) must be conducted because the scan
8 ranges of the radar sites overlap. Because the maximum value method is applied to merge
9 radar rainfalls by the KMA (Korea Meteorological Administration, 2012b), the identical
10 method is also utilized in this paper.

11

12 [Figure 2. Flowchart of the Radar-AWS Rainrate calculation system]

13

14 **2.3 Bias Correction Methods**

15 **2.3.1 Reflectivity Measurement Bias Correction Method**

16 Weather radars continuously carry out measurement cycles which include sending signals
17 into the atmosphere and receiving and analyzing return signals for meteorological observation.
18 The measurement of reflectivity itself suffers from hardware malfunctions (e.g. electronic
19 miscalibration, signal misprocessing) and radar characteristics (e.g. attenuation). When
20 converting radar reflectivity into rainrates (Z-R relationship) leads to additional bias which

1 can lower the accuracy of rainfall estimation. To estimate the Z -bias of target weather radars,
2 a reference weather radar which has been absolutely corrected is required. The Z -bias is
3 defined as the difference between the measured reflectivity of reference radar and the target
4 radar under the same spatial and temporal conditions (Weather Radar Center, 2012). The
5 procedure of estimating Z -bias is described as follows.

6

7 ***(a) Calibration of the reference weather radar***

8 This paper selected a Bislsan S-band dual-polarimetric radar (hereafter Bislsan dual-pol
9 radar) which can be self-calibrated and is more accurate than the reference weather radar. To
10 calibrate the Bislsan dual-pol radar, a self-consistency constraint method using the
11 relationship between the reflectivity (Z) depended by the radar beam power and the specific
12 differential phase (K_{DP}) affected by only particle size or concentration, not the radar beam
13 power was utilized. The procedure of the self-consistency constraint method is as follows
14 (Weather Radar Center, 2012):

15 (i) Derive the Z_H - K_{DP} relationship theoretically from the Drop Size Distributions (DSDs)

16 (ii) Calculate K_{DP} for each radar pixel from observed Z_H using the derived Z_H - K_{DP}
17 relationship and Φ_{DP} as integrating calculated K_{DP} along each radial

18 (iii) Calculate the difference angle (θ) using a scatter plot between the calculated Φ_{DP} from
19 (ii) and observed from the Bislsan dual-pol radar and calculate Z -bias (ε) by inputting

1 the difference angle (θ) into Equation (3) and (4) (Lee, et al., 2006) (refer to Figure
2 3)

3

4
$$\tan \theta = \frac{\sum_{i=1}^n (\Phi_{DP_cal} - \Phi_{DP_obs})}{\sum_{i=1}^n \Phi_{DP_obs}^2} \quad (3)$$

5 $\varepsilon(dB) = 10b \log(\tan \theta) \quad (4)$

6

7 Where, Φ_{DP_cal} is theoretical Φ_{DP} from DSDs, Φ_{DP_obs} is observed Φ_{DP} from the dual-pol radar,
8 θ is the difference angle, b is the empirical constant, and ε is the estimated Z-bias.

9

10 [Figure 3. Example for the procedure of the self-consistency constraint: Calculation of $\tan \theta$
11 using Equation (3)]

12

13 ***(b) Calculation of Z-bias for the target weather radars***

14 After completed to calibrate the Bislsan dual-pol radar for Z-bias, target single-pol radars
15 which are located adjacent to the reference radar were calibrated according to the reflectivity

1 of the reference radar. The procedure for calculating the Z-bias of the target radars is as
2 follows (Korea Meteorological Administration, 2011):

3

4 (i) Remove the beam-blockage area using beam-blockage information (penetration ratio
5 more than 90%)

6 (ii) Reflect the accumulated attenuation effects due to rainfall in the observed reflectivity
7 (attenuation ratio less than 10%)

8 (iii) Generate the 3-dimensional CAPPI for the reflectivity

9 (iv) Set up equidistant pairs between the reference and target radars within 200 km from
10 the center of the reference radar (However, when a Bislsan dual-pol radar was a
11 reference radar, the distance was within 100 km)

12 (v) Compare the reflectivity of the reference and target radars within a ± 5 km reflectivity
13 overlap area

14 (vi) Calculate the reflectivity differences at intervals of 0.5 km from 1.5~3.5 km altitude in
15 consideration of the ground clutter and bright band and average the reflectivity
16 differences for the Z-bias of the target radar

17

1 Figure 4 shows the concept of Z-bias for target radar which has been calculated from
2 reflectivity differences in the overlap area between the reference and target radars. After
3 completed to calibrate the target radar#1 for the Z-bias, the target radar#1 is the reference
4 radar for the target radar#2 adjacent to the target radar#1. The procedure mentioned above is
5 equally applied for the target radar#1 and #2 to calculate the Z-bias of target radar#2.

6

7 [Figure 4. The concept of calculating Z-bias for the target radar according to the reference
8 radar reflectivity (Korea Meteorological Administration, 2011)]

9

10 **2.3.2 Rainfall Bias Correction Methods**

11 Estimated rainfall based on radars has the QPE model bias (parameters of Z-R relationship,
12 parameters of QPE model, QPE model structures, etc.) even if calibrated reflectivity is input
13 into the QPE model. In this paper, the Mean Field Bias Correction (MFBC) method and Local
14 Gauge Correction (LGC) method have been applied to outcomes from the QPE model for
15 correcting the rainfall-bias.

16

17 **(a) Mean Field Bias Correction method**

18 The fundamental concept of the MFBC method is that the bias correct factor (G/R ratio
19 factor) is calculated using the ratio of the spatial average (mean) between rainfalls estimated

1 from radars and observed rainfall at a corresponding field (or point, pixel). Then corrected
2 rainfall is calculated by multiplying the G/R ratio factor and radar rainfall estimates. The
3 equation of the MFBC method is as follows:

4

5
$$\text{G/R ratio factor} = \frac{\sum_{i=1}^n G_i}{\sum_{i=1}^n R_i} \quad (5)$$

6

7 Where, G_i is rainfall of i^{th} rain gauge, R_i is radar rainfall estimates of i^{th} point (or pixel), n is
8 the total number of the ground rain gauge. In the case of utilizing the MFBC method in a
9 certain area (or for a certain period), the identical G/R ratio factor is uniformly applied to
10 radar rainfall estimates all over the area.

11

12 ***(b) Local Gauge Correction method***

13 This study dealt with the Local Gauge Correction (LGC) method which has been
14 employed in the NMQ (National Mosaic and QPE) of the NOAA (National Oceanic and
15 Atmospheric Administration) NSSL (National Severe Storms Laboratory) (Zhang *et al.*,
16 2011). The LGC method which assigns the weights to bias between ground rainfall detected
17 by AWSs and radar rainfall estimates is the modified version of the Inverse Distance
18 Weighting (IDW) method. The LGC method is able to correct the rainfall cases which occur
19 locally by modifying rainfall estimates in each pixel. The procedure of the LGC method is as
20 follows (refer to Figure 5):

1 This paper defined that $r_{LGC,i}$ is the corrected rainfall estimates in a certain point i , r_i is
2 radar rainfall estimates in a certain radar pixel i , $R_{e,i}$ is expected error estimates. This
3 relationship is expressed as following equation:

4

5 STEP 1: $r_{LGC,i} = r_i - R_{e,i} = r_{LGC,i}(b, D)$ (6)

6

7 Where D is effective radius for calculating the radar rainfall bias, b is the weight of variable d ,
8 d is the distance between AWSs and pixels in radars. Estimated weights by Equation (7) are
9 applied to Equation (6) (Zhang *et al.*, 2011).

10

11
$$R_{e,i} = \sum_{j=1}^m e_j w_j / \sum_{j=1}^m w_j$$
 (7)

12

13 If general, $w_j = 1/d_j^b$ (if $d_j \leq D$) or 0 (if $d_j > D$)

14 If the number of AWS in region are sparse, $\alpha = \sum_{j=1}^m \exp[-d_j^2 / (D/2)^2]$ (8)

15 ; $w_j = \alpha \times 1/d_j^b$ (if $d_j \leq D$) or 0 (if $d_j > D$)

16

17 Where e_j is error between rainfalls observed from AWSs (g_j) and radar rainfall estimates (r_j),
18 w is the weight of error ($=r_j - g_j$), j is j^{th} AWS, m is the number of AWSs within the effective
19 radius, α is the impact factor. If the α is more than one, the number of AWSs is enough for
20 the rainfall-bias correction. Otherwise, less than one, if the number of AWSs is sparse (the α

1 is less than one), revised weights have been calculated by multiplying α and original weights
2 ($w_j = \alpha \times 1/d_j^2$).

3 E_i is defined as the difference between r_{LGC} from STEP 1 and ground rainfall, g_i and
4 depends on b and D .

5

6 STEP 2: $E_i = r_{LGC} - g_i = E_i(b, D)$ (9)

7

8 Mean Square Error (MSE) for E_i is expressed as Equation (10) and also depends on
9 parameter b and D . Parameters of the LGC method (b and D) have been determined using the
10 stepwise method for minimizing the MSE value and applied to Equation (8) to calculate radar
11 rainfall estimates, r_{LGC} .

12

13 STEP 3: $MSE = \sum_{i=1}^n E_i^2 / n = MSE(b, D)$ (10)

14

15 This paper has assumed that the scan range of radars (D) is the maximum range 240 km
16 used by all AWSs on the Korean Peninsula. Although it takes a long time to carry out the
17 LGC algorithm under this assumption, it is considered appropriate to verify the improvement
18 of radar rainfall estimates using the LGC method.

19 In sequence, because the LGC method is highly dependent on the number of AWSs which
20 are available and accurate, the quality control algorithm for AWSs has been conducted to
21 remove lower-quality AWSs which have larger expected errors than others. The conditions of

1 quality control are as follows: (i) In a certain AWS, if the number of pixels which have $D_{R,E}$
2 less than 5 mm are less than 25% of the whole pixels, a certain AWS is designated as an
3 ‘abnormal AWS’ and removed. $D_{R,E}$ are the differences between $R_{e,i}$ and E_i within 10-km
4 radius from the center of a certain AWS. (ii) The LGC method has been conducted until the
5 number of available AWSs was more than 90% of all the filtered AWSs. If this procedure is
6 stopped, calculated r_{LGC} at the present stage is used for corrected rainfall estimates. (iii) The
7 procedure of the LGC method is finally finished after repeating the routine above
8 approximately four times. Furthermore, if the ratio of abnormal AWSs is more than 7%, the
9 procedure of the LGC method is also finished (Korea Meteorological Administration, 2012).
10 Thresholds were decided using the stepwise method and are appropriate for the LGC method
11 applied to the RAR calculation system. However the thresholds are somewhat subjective, it is
12 considered that future studies should deal with this limitation.

13

14 [Figure 5. Flowchart of the Local Gauge Correction method]

15

16 **3. APPLICATION AND RESULTS**

17 **3.1 Application of the Reflectivity Measurement Bias Correction method**

18 In section 2.2.1, the Reflectivity measurement bias (Z-bias) for the Bislsan dual-pol radar
19 have been estimated using the self-consistency constraint method using the relationship
20 between reflectivity (Z) and specific differential phase (K_{DP}) during the calibration period.

1 The Z-bias of the Bislsan dual-pol radar was estimated as -2.61 dB with the result that the
2 calculated $\tan\theta$ which was 0.58 degree from Equation (1) was inputted into Equation (4). The
3 Bislsan dual-pol radar was self-calibrated using its Z-bias. For estimating the Z-bias of target
4 radars, first of all, pairs between the reference radar and target radar were set up (refer to
5 Table 2). Then averaged Z-biases of the 11 single-pol radars operated by the KMA as target
6 radars were estimated sequentially from the beginning, using the Bislsan dual-pol radar as the
7 reference radar (refer to Figure 6 and Table 3). The Z-biases of the BRI and JNI sites were -
8 7.87 dB (the largest) and -1.16 dB (the smallest) and Z-bias on average was -4.52 dB.
9 Especially, radar rainfall estimates were underestimated due to the fact that all of the Z-biases
10 had negative values.

11 To verify the improvement of radar rainfall estimates, the RAR system which reflected the
12 Z-biases of all the radar sites were conducted to calculate rainfall estimates of 18 cases in the
13 summer season. In Figure 7, after applying Z-biases to the RAR system, the accuracy of
14 rainfall estimates improved in the Root Mean Square Error (RMSE) and correlation
15 coefficient, which ranged from 7.37 mm hr^{-1} and 0.83 and 7.21 mm hr^{-1} and 0.84 on average,
16 respectively. As a result of each rainfall type, in RMSE, the accuracy of rainfall estimates in
17 Changma front cases was improved from 7.43 mm hr^{-1} to 7.36 mm hr^{-1} and the accuracy of local
18 torrential rainfall cases (7.43 mm hr^{-1}) was similar to results without the application of Z-bias
19 (7.36 mm hr^{-1}). Especially, the accuracy of typhoon cases deteriorated compared to existing
20 results (from 9.08 mm hr^{-1} to 11.04 mm hr^{-1}). This was due to the application of Z-biases to each radar
21 site in the RAR system, which has increased the rainfall estimates in whole country. The
22 accuracy of Changma front cases which occur nationwide was improved. However, because

1 cases of local torrential rainfalls and typhoons occurred locally, the accuracy of these cases
2 was negatively impacted. In Figure 8 in Case 12 at 1500 LST on 10 August in 2012, Figure
3 8(a) shows the image before the application of Z-bias and Figure 8(b) shows the image after
4 the Z-bias correction. Rainfall estimates in black dash circles on the partial magnification
5 image in Figure 8(b) are stronger than Figure 8(a), relatively since the rainfall estimates were
6 increased by the Z-bias correction. It is proved that the Z-bias correction proposed by this
7 paper has improved the accuracy of rainfall amounts in the RAR system.

8

9 [Table 2. Radar pairs for estimating the Z-bias of each radar site]

10 [Figure 6. Sequence of the reflectivity bias estimation for each radar site]

11 [Table 3. Reflectivity bias for each radar site]

12 [Figure 7. Comparison of the accuracy of rainfall estimates for each rainfall case before and
13 after the Z-bias correction: (a) RMSE; (b) correlation coefficient]

14 [Figure 8. Comparison of rainfall estimate images in the RAR system before and after the Z-
15 bias correction in Case 12 (at 1500 LST on 10 August in 2012): (a) Before the Z-bias
16 correction; (b) After the Z-bias correction]

17

18 **3.2 Application of the QPE Model Bias Correction methods**

1 Since the rainfall estimates in the RAR system were improved by the Z-bias correction in
2 Section 3.1, the QPE model bias (rainfall-bias) correction was conducted after the Z-bias
3 correction. To verify the improvement of the radar rainfall amounts estimated by the QPE
4 model bias correction, the RAR system with rainfall-bias correction was conducted for 18
5 summer season cases over the verification period. This paper defined that results with only
6 the Z-bias correction were identified as ‘Z-bias’, results with the Z-bias correction and MFBC
7 method were identified as ‘Z-bias_MFBC’, and results with the Z-bias correction and LGC
8 method were identified as ‘Z-bias_LGC’.

9 As a result of the rainfall-bias correction methods, Table 4 shows the accuracy of rainfall
10 estimates for each rainfall-bias method and for each rainfall type. In Table 4(a), Mean
11 Absolute Error (MAE) of the Z-bias, Z-bias_MFBC, and Z-bias_LGC were 3.65, 3.37, and
12 2.19 mm hr⁻¹, respectively. Among them, the accuracy of the Z-bias_LGC was superior to the
13 others. In RMSE, the accuracy of rainfall amounts of the RAR system was improved by about
14 7.4% (from 7.21 to 6.68 mm hr⁻¹) in the Z-bias_MFBC and 63.7% (from 7.21 to 2.62 mm hr⁻¹)
15 in the Z-bias_LGC. In correlation coefficient, the accuracy of the RAR system was also
16 improved by about 10.7% (from 0.84 to 0.93) in Z-bias_MFBC and 11.7% (from 0.84 to 0.94)
17 in Z-bias_LGC. It is proved that the accuracy of rainfall estimates in the RAR system was
18 improved by the Z-bias with rainfall-bias correction methods more than only the Z-bias.
19 Especially, among the rainfall-bias correction methods, the Z-bias_LGC is superior to others.
20 The reason is that although the same rainfall-bias was applied to the overall application region
21 in the MFBC method, the different rainfall biases were applied to each rainfall amount by
22 radar pixel in the LGC method. In Table 4(b), although correlation coefficients in the Z-bias

1 correction were similar to all rainfall types, typhoon cases had the lowest accuracy in RMSE.
2 As a result of the Z-bias_MFBC, correlation coefficients in all types were improved when
3 compared with Z-bias. While the accuracy of the Z-bias_MFBC in RMSE improved over the
4 Z-bias except for in Changma front cases, results of typhoon cases were inferior to others as
5 always. Results of the Z-bias_LGC showed that the accuracy of rainfall estimates for all types
6 in RMSE and correlation coefficients was superior to the Z-bias and, especially, outcomes in
7 typhoon cases were vastly superior to the others. Figure 9 has explained that the RMSEs of
8 the Z-bias_LGC of all cases were outstanding in Figure 9(a) and while correlation coefficients
9 of the Z-bias_MFBC were not much different to the Z-bias_LGC on average, only the Z-bias
10 correction results were generally lower in Figure 9(b).

11 Figure 10 shows rainfall estimate images of AWS, Z-bias, Z-bias_MFBC, and Z-
12 bias_LGC in Case 12 (at 1500 LST on 10 August in 2012) and Case 18 (at 1100 LST on 30
13 August in 2012). In Figure 10(a) in Case 12, the maximum rainfall amount in AWSs was 48.0
14 mm/hr⁻¹ and the black arrows indicate the strongest rainfall fields. Figure 10(b) shows that
15 since the displayed rainfall regions were similar to AWSs, rainfall amounts were
16 underestimated in the whole area. As an image of the Z-bias_MFBC in Figure 10(c), rainfall
17 amounts in a black circle were closer to AWSs than Figure 10(b). Especially, the image of the
18 Z-bias_LGC is similar to AWSs and rainfall estimates which ranged from 40 to 50 mm hr⁻¹ in
19 the regions, indicated by black arrows in a black circle were similar to AWSs. In Figure 11(a)
20 in Case 18, the maximum rainfall amount in AWSs was 54.0 mm hr⁻¹ and the rainfall fields
21 indicated by black arrows were stronger than the others. Particularly, the rainfall zones (the
22 black dash line) from the southwest to the northeast occurred due to the direct effects of the

1 typhoon Tembin along its track (the purple line). Figure 11(b) shows rainfall amounts in only
2 the Z-bias were much underestimated in whole area. By contrast, in Figure 11(c) for the Z-
3 bias_MFBC, the maximum rainfall estimates in a region ① which was located in the
4 southeast of the Tembin and in rainfall zones from the southwest to the northeast (region ②)
5 were much improved. However, rainfall estimates in region ① were a little underestimated
6 and the region ② had slightly strong rainfall amounts. In Figure 11(d), since rainfall estimates
7 in region ③ were stronger than for region ① and the region ④ had lighter rainfall amounts
8 than the region ②, an image of rainfall estimates in the Z-bias_LGC was coterminous with
9 AWSs. It is proved that the accuracy of the rainfall estimates in the RAR system with the
10 rainfall-bias correction is improved compare to using only the Z-bias correction. Especially,
11 the Z-bias_LGC is superior to the others.

12

13 [Table 4. Application results of the QPE Model Bias Correction methods]

14 [Figure 9. Comparison of the rainfall estimation accuracy for each rainfall in the Z-bias, Z-
15 bias_MFBC, and Z-bias_LGC methods: (a) RMSE; (b) correlation coefficient]

16 [Figure 10. Comparison of the rainfall images between the AWS and Model Bias Correction
17 method results in Case 12 (at 1500 LST on 10 August in 2012): (a) the AWS; (b) the OBC
18 method; (c) the OBC_MFBC method; (d) the OBC_LGC method]

1 [Figure 11. Comparison of the rainfall images between the AWS and Model Bias Correction
2 method results in Case 18 (at 1100 LST on 30 August in 2012): (a) the AWS; (b) the OBC
3 method; (c) the OBC_MFBC method; (d) the OBC_LGC method]

4

5 **4. CONCLUSIONS**

6 This paper focuses on correcting the reflectivity measurement bias (Z-bias) which includes
7 temporal and spatial sampling bias, ground and sea clutter, beam-blockage and attenuation,
8 electrical calibration, and quantification of reflectivity bias and the QPE model bias (rainfall-
9 bias) which includes bias due to the parameters of Z-R relationship, parameters of the QPE
10 model, and the QPE model structure to improve radar rainfall estimates. The reference radar,
11 Bislsan S-band dual-polarimetric radar, which was self-calibrated with the self-consistency
12 constraint method using the relationship between Z and K_{DP} was utilized to calculate the Z-
13 biases of all target radar sites and Z-biases were applied to the QPE model, RAR system. The
14 MFBC and LGC methods which correct rainfall-biases have also been applied to the RAR
15 system to improve the accuracy of radar rainfall estimates.

16 As a result of the Z-bias correction in 18 summer season cases, the accuracy of rainfall
17 estimates improved in the RMSE and correlation coefficient which ranged from 7.37 mm hr^{-1}
18 and 0.83 and 7.21 mm hr^{-1} and 0.84 on average, respectively and, for rainfall types, the
19 accuracy of rainfall estimates in Changma front and local torrential cases was slightly
20 improved or similar to results without the application of Z-bias. Especially, the accuracy of
21 typhoon cases was worse than existing results (from 9.08 to 11.04 mm hr^{-1}). The reason is that

1 the application of Z-biases to each radar site in the RAR system has increased the rainfall
2 estimates for the whole country. The accuracy of Changma front cases, which occur
3 nationwide, was improved. However, because cases of torrential rainfalls and typhoon have
4 occurred locally, the accuracy of these cases was worsened. In comparison with rainfall
5 images, rainfall estimates with the Z-bias correction have been established to be stronger to
6 existing image.

7 Since the rainfall estimates in the RAR system has been improved by the Z-bias correction,
8 the QPE model bias (rainfall-bias) correction was conducted after the Z-bias correction. For
9 results of the rainfall-bias correction methods, the accuracy of rainfall estimates with the Z-
10 bias_MFBC was improved by about 7.4% in RMSE and 10.7% in correlation coefficient in
11 comparison with only the Z-bias, respectively, and the accuracy of the Z-bias_LGC was
12 especially superior to the others (63.7% in RMSE and 11.7% in correlation coefficient). The
13 reason is that although the same rainfall-bias was applied to the all over area in the MFBC
14 method, the different rainfall biases were applied to each rainfall amount by radar pixel in the
15 LGC method. For rainfall types, results of the Z-bias_LGC showed that the accuracy of
16 rainfall estimates for all types in RMSE and correlation coefficient was much improved over
17 only the Z-bias and, especially, outcomes in typhoon cases were vastly superior to the others.
18 In comparison of rainfall images, rainfall estimates with the Z-bias_LGC were determined to
19 closer to AWSs in the cases of Changma fronts and the typhoon, Tembin.

20 Therefore, in this paper, it is proved that the accuracy of the rainfall estimates in the RAR
21 system, to which the Z-bias correction and rainfall-bias correction method (MFBC and LGC)

1 were applied, has been improved. These bias correction methods proposed by this paper are
2 able to contribute to the real-time QPE model, the RAR system, in work-site operation and
3 to fundamental bias correction research. However, this paper has dealt with the bias
4 corrections in a few parts in a series of a procedure. Since radar rainfall estimates are still
5 based on a series of assumptions, more research on numerous systematic biases, also
6 including natural biases, should be undertaken the performance of the calculation of radar-
7 based rainfall estimates.

8

9 **Acknowledgements:** This research is supported by "Development and application of Cross
10 governmental dual-pol radar harmonization (WRC-2013-A-1)" project of the Weather Radar
11 Center, Korea Meteorological Administration in 2014 and Deajin University.

12

13

14

15

16

17

18

1 **References**

2 Austin, P.M., 1987: Relation between measured radar reflectivity and surface rainfall.
3 *Monthly Weather Review*, **115**, 1053–1070.

4 Campos, E., and I. Zawadzki, 2000: Instrumental uncertainties in Z – R relations. *Journal of*
5 *Applied Meteorology*, **39**, 1088–1102.

6 Chumchean S., Sharma, A., and Seed, A., 2006: An integrated approach to error correction
7 for real-time radar-rainfall estimation. *Journal of Atmospheric and Oceanic Technology*,
8 **23**, 67-79.

9 Ehret, U. 2002: Rainfall and flood nowcasting in small catchments using weather radar. PhD
10 Thesis, University of Stuttgart.

11 Germann, U., Galli, G., Boscacci, M., and Bolliger, M., 2006: Radar precipitation
12 measurement in a mountainous region. *Quarterly Journal of the Royal Meteorologic*
13 *Society*, **132**, 1669–1692.

14 Huff, F.A., 1970: Sampling errors in measurement of mean precipitation. *Journal of Applied*
15 *Meteorology*, **9**, 35–44.

16 Jeong, J., Yu, M., and Yi, J., 2014: Runoff analysis using dual polarization radar and
17 distributed model, *Journal of Korea Water Resources Association*, **47**, 801-812.

18 Jordan, P., Seed, A., Austin, G., 2000: Sampling errors in radar estimates of rainfall. *Journal*
19 *of Geophysical Research: Atmospheres*, **105**, 2247–2257.

20 Kim, D.-S., Kang, M.-Y., Lee, D.-I., Kim, J.-H., Choi, B.-C., and Kim, K. E., 2006:
21 Reflectivity Z and differential reflectivity ZDR correction for polarimetric radar rainfall

1 measurement. *Proceeding of the Spring Meeting of Korean Meteorological Society*, 130-
2 131.

3 Kim, J.-B., Choi, W.-S., and Bae, D.-H., 2015: Assessment of dual-polarization radar for
4 flood forecasting, *Journal of Korea Water Resources Association*, **48**, 257-268.

5 Korea Meteorological Administration, 2011: *Development of collaboration management*
6 *system for radar data (I)*. Weather Radar Center.

7 Korea Meteorological Administration, 2012a: *Development of Radar-based Multi-sensors*
8 *Quantitative Precipitation Estimation Technique Report*, Weather Radar Center.

9 Korea Meteorological Administration, 2012b: *Radar rainfall estimation comparison and*
10 *verification joint experiment report*. Weather Radar Center and Meteorological
11 Advancement Council, Korea Meteorological Administration.

12 Krajewski, W.F., Smith, J., 2002: Radar hydrology: rainfall estimation. *Advanced Water*
13 *Resources*. **25**, 1387–1394.

14 Lee, G.W. 2006: Sources of errors in rainfall measurements by polarimetric radar: variability
15 of drop size distributions, observational noise, and variation of relationships between R
16 and polarimetric parameters. *Journal of Atmospheric and Oceanic Technology*, **23**, 1005-
17 1028.

18 Marshall, J.S. and Palmer, W.M. 1948: The distribution of raindrops with size. *Journal of*
19 *Meteorology*, **5**, 165-166.

20 McMillan, H., Jackson, B., Clark, M., Kavetski, D., and Woods, R. 2011: Rainfall uncertainty
21 in hydrological modeling: An evaluation of multiplicative error models, *Journal of*
22 *Hydrology*, **400**, 83-94.

1 Morin, E. and Gabella, M., 2007: Radar-based quantitative precipitation estimation over
2 Mediterranean and dry climate regimes. *Journal of Geophysical Research*, **112**,
3 D20108.doi:10.10029/2006JD008206.

4 Moulin, L., Gaume, E., Obled, C., 2009: Uncertainties on mean areal precipitation:
5 assessment and impact on streamflow simulations. *Hydrology and Earth System Sciences*,
6 **13**, 99–114.

7 Oh, H.-M., Ha, K.-J, Kim, K.-E., and Bae, D.-H. 2003: Precipitation rate combined with the
8 use of optimal weighting of radar and rain gauge data. *Atmosphere, Korean
9 Meteorological Society*, **13**, 316-317.

10 Rosenfeld, D., Wolff, D.B., and Atlas, D., 1993: General probability-matched relations
11 between radar reflectivity and rain rate, *Journal of Applied Meteorology*, **32**, 50-72.

12 Sinclair, S. and Pegram, G. 2005: Combining radar and rain gauge rainfall estimates using
13 conditional merging. *Atmospheric Science Letters*, **6**, 19-22.

14 Villarini, G., 2008: *Empirically-based modeling of radar-rainfall uncertainties*. Ph.D. thesis,
15 The University of Iowa, 321.

16 Villarini, G., and Krajewski, W.F., 2008: Empirically-based modeling of spatial sampling
17 uncertainties associated with rainfall measurements by rain gauges. *Advanced Water
18 Resources.*, **31**, 1015–1023.

19 Villarini, G., and Krajewski, W.F., 2010: Sensitivity studies of the models of radar-rainfall
20 uncertainties. *Journal of Applied Meteorology and Climatology*, **49**, 288-309.

1 Villarini, G., Mandapaka, P.V., Krajewski, W.F., and Moore, R. J., 2008: Rainfall and
2 sampling errors: A rain gauge perspective. *Journal of Geophysical Research*, **113**,
3 D11102, doi:10.1029/2007JD009214.

4 Weather Radar Center, 2013. *Development of integrated quality control algorithm for Korean*
5 *radar data*. Korea Meteorological Administration.

6 Wilson, J.W., Brandes, E.A., 1979: Radar measurement of rainfall. *Bulletin of American*
7 *Meteorological Society*, **60**, 1048–1058.

8 Woodley, W., Olsen, A., Herndon, A., and Wiggert, V., 1975: Comparison of gage and radar
9 methods of convective rain measurement. *Journal of Applied Meteorology*, **14**, 909–928.

10 Yoo, C., Kim, J., Yoon, J., Park, C., Park, C., and Jun, C., 2011: Use of the Kalman filter for
11 the correction of mean-field bias of radar rainfall, *The 5th Korea-Japan-China Joint*
12 *Conference on Meteorology*, Busan, Korea.

13 You, C.-H., Lee, D.-I., and Kang, M.-Y., 2014: Rainfall estimation using specific differential
14 phase for the first operational polarimetric radar in Korea, *Advances in Meteorology*,
15 Article ID 413717. <http://dx.doi.org/10.1155/2014/413717>.

16 Zhang, J., Howard, K., Langston, C., Vasiloff, S., Kaney, B., Arthur, A., Cooten, V.C.,
17 Kelleher, K., Kitzmiller, D., Ding, F., Seo, D.-J., Wells, E., and Dempsey, C., 2011:
18 National mosaic and multi-sensor QPE(NMQ) system: Description, results, and future
19 plans. *Bulletin of the American Meteorological Society*, **92**, 1321-1338.

20 Zhang, Y., Adams, T., and Bonta, J.V., 2007: Subpixelscale rainfall variability and the effects
21 on the separation of radar and gauge rainfall errors. *Journal of Hydrometeorology*, **8**,
22 1348–1363.

1 **Table captions**

2 **Table 1.** Summary of the Radars and Rainfall Cases

3 **Table 2.** Radar pairs for estimating the Z-bias of each radar site

4 **Table 3.** Reflectivity bias for each radar site

5 **Table 4.** Application results of the QPE Model Bias Correction methods

6

7

8

9

10

11

12

13

14

15

16

17

18

19

20

21

1 List of Figures

Fig. 1. Location of 11 single-polarization radars and the Bislsan S-band dual-polarization radar and their observation ranges

4 **Fig. 2.** Example for the procedure of the self-consistency constraint: Calculation of $\tan \theta$
 5 using equation (1)

6 **Fig. 3.** The concept of calculating Z-bias for the target radar according to the reference radar
7 reflectivity (Korea Meteorological Administration, 2011)

8 **Fig. 4.** Flowchart of the Local Gauge Correction method

9 **Fig. 5.** Flowchart of the Radar-AWS Rainrate calculation system

10 **Fig. 6.** Sequence of the reflectivity bias estimation for each radar site

11 **Fig. 7.** Comparison of the accuracy of rainfall estimates for each rainfall case before and after
12 the Z-bias correction: (a) RMSE; (b) correlation coefficient

13 **Fig. 8.** Comparison of rainfall estimate images in the RAR system before and after the Z-bias
14 correction in Case 12 (at 1500 LST on 10 August in 2012): (a) Before the Z-bias
15 correction; (b) After the Z-bias correction

16 **Fig. 9.** Comparison of the rainfall estimation accuracy for each rainfall in the Z-bias, Z-
 17 bias MFBC, and Z-bias LGC methods: (a) RMSE; (b) correlation coefficient

1 **Fig. 10.** Comparison of the rainfall images between the AWS and Model Bias Correction
2 method results in Case 12 (at 1500 LST on 10 August in 2012): (a) the AWS; (b) the
3 OBC method; (c) the OBC_MFBC method; (d) the OBC_LGC method

4 **Fig. 11.** Comparison of the rainfall images between the AWS and Model Bias Correction
5 method results in Case 18 (at 1100 LST on 30 August in 2012): (a) the AWS; (b) the
6 OBC method; (c) the OBC_MFBC method; (d) the OBC_LGC method

7

8

9

10

11

12

13

14

15

16

17

18

19

20

21

22

1 **Table 1.** Summary of the Radars and Rainfall Cases

2 (a) Summary of the radars and rainfall data used for calculating observational biases

Items	Details
Reference radar	Bislsan S-band dual-polarization radar (Maximum observation range: 150 km; Gate size: 0.125 km; Elevation: 6 angles; Update: every 2.5 minute interval)
Target radar	11 single-polarization radars operated by the Korea Meteorological Administration: Baegnyeondo (BRI, S-band), Kwanaksan (KWK, S-band), Oseonsan (KSN, S-band), Jindo (JNI, S-band), Gosan (GSN, S-band), Seongsan (SSP, S-band), Gudeoksan (PSN, S-band), Myeonbongsan (MYN, C-band), Gangneung (GNG, S-band), Gwnagdeoksan (GDK, S-band), Incheon (IIA, C-band)
Calibration data	Rainfall cases from 1 June to 31 August in 2012

3

4

5

1 (b) Rainfall cases used for verification of the observational and model bias correction

Items	Period (LST)	Sources
Case 1	20120608 0600 - 20120608 1900	Local torrential rainfalls
Case 2	20120615 0500 - 20120616 0400	Changma front
Case 3	20120618 0000 - 20120619 1300	Changma front
Case 4	20120623 1300 - 20120624 1900	Local torrential rainfalls
Case 5	20120629 0800 - 20120701 0100	Changma front
Case 6	20120705 0400 - 20120707 0200	Changma front
Case 7	20120710 1000 - 20120711 1900	Changma front
Case 8	20120712 2330 - 20120713 0730	Changma front
Case 9	20120714 0800 - 20120715 1500	Changma front
Case 10	20120716 2300 - 20120717 2200	Changma front
Case 11	20120718 1400 - 20120719 1300	Typhoon
Case 12	20120810 0300 - 20120810 2200	Local torrential rainfalls
Case 13	20120812 0500 - 20120813 1500	Local torrential rainfalls
Case 14	20120814 1700 - 20120816 2300	Local torrential rainfalls
Case 15	20120819 1600 - 20120822 2100	Local torrential rainfalls
Case 16	20120822 2200 - 20120825 1100	Local torrential rainfalls
Case 17	20120827 1300 - 20120828 1800	Changma front and Typhoon
Case 18	20120829 1500 - 20120830 2300	Typhoon

2

3

1 **Table 2.** Radar pairs for estimating the Z-bias of each radar site

Reference radar	Target radar	Reference radar	Target radar
BSL	KSN, PSN, MYN	IIA	BRI
KSN	JNI	KSN	KWK
JNI	GSN, SSP	KWK	GDK
KWK	IIA	GDK	GNG

2

3

4

5

6

7

8

9

10

11

1 **Table 3.** Reflectivity bias for each radar site

Radar site	Reflectivity bias (dB)	Radar site	Reflectivity bias (dB)
BRI	-7.87*	JNI	-1.16
GDK	-4.29	KSN	-4.87
GSN	-3.99	KWK	-5.15
GNG	-4.77	MYN	-5.63
IIA	-5.19	PSN	-2.28
SSP	-4.50		

2 * Average reflectivity bias during the calibration period

3
4
5
6
7
8
9
10
11
12
13

1 **Table 4.** Application results of the QPE Model Bias Correction methods

2 (a) Total average

Method	MAE (mm hr ⁻¹)	RMSE (mm hr ⁻¹)	Correlation coefficient
Z-bias	3.65	7.21	0.84
Z-bias_MFBC	3.37	6.68 (7.4%*)	0.93 (10.7%)
Z-bias_LGC	2.19	2.62 (63.7%)	0.94 (11.7%)

3 * represents the change ratio related to the OBC method in RMSE and correlation coefficient

4

5 (b) Average for each rainfall type

Method	Types	Averaged RMSE (mm hr ⁻¹)	Averaged correlation coefficient
Z-bias	Changma front	5.64	0.87
	Local torrential rainfall	7.36	0.81
	Typhoon	11.04	0.83
Z-bias_MFBC	Changma front	5.75	0.93
	Local torrential rainfall	6.74	0.95
	Typhoon	9.00	0.86
Z-bias_LGC	Changma front	2.49	0.95
	Local torrential rainfall	2.69	0.94
	Typhoon	2.81	0.93

6

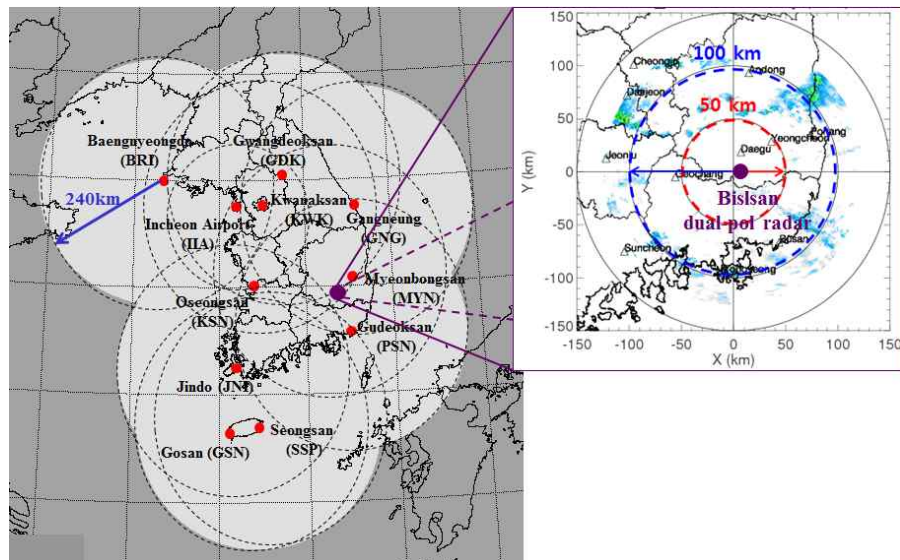
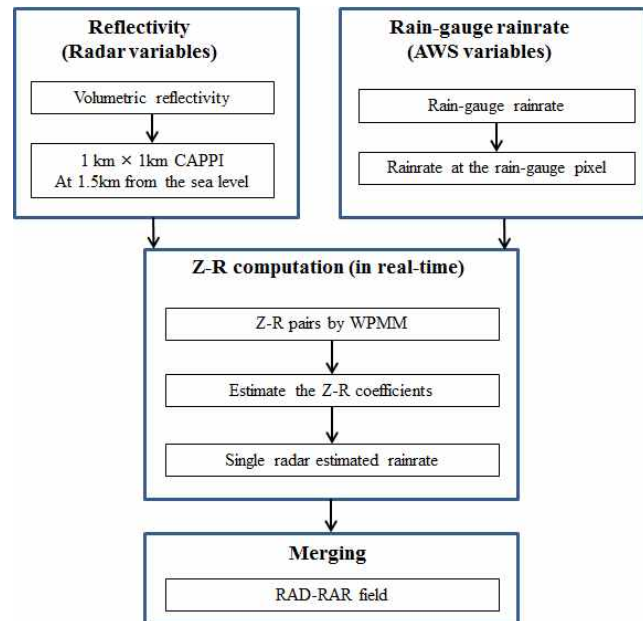


Fig. 1. Location of 11 single-polarization radars and the Bislsan S-band dual-polarization radar and their observation ranges



1

2 **Fig. 2.** Flowchart of the Radar-AWS Rainrate calculation system

3

4

5

6

7

8

9

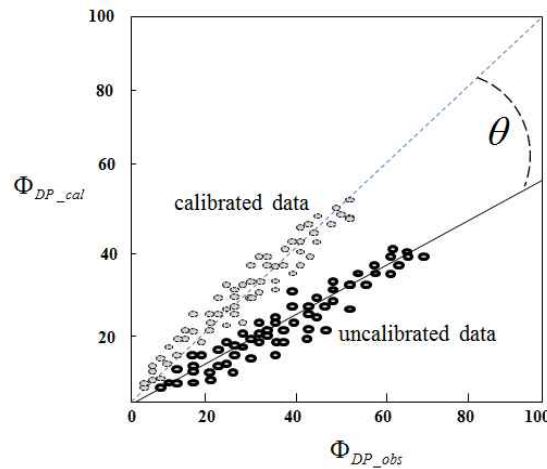
10

11

12

13

14



1

2 **Fig. 3.** Example for the procedure of the self-consistency constraint: Calculation of $\tan \theta$
 3 using equation (3)

4

5

6

7

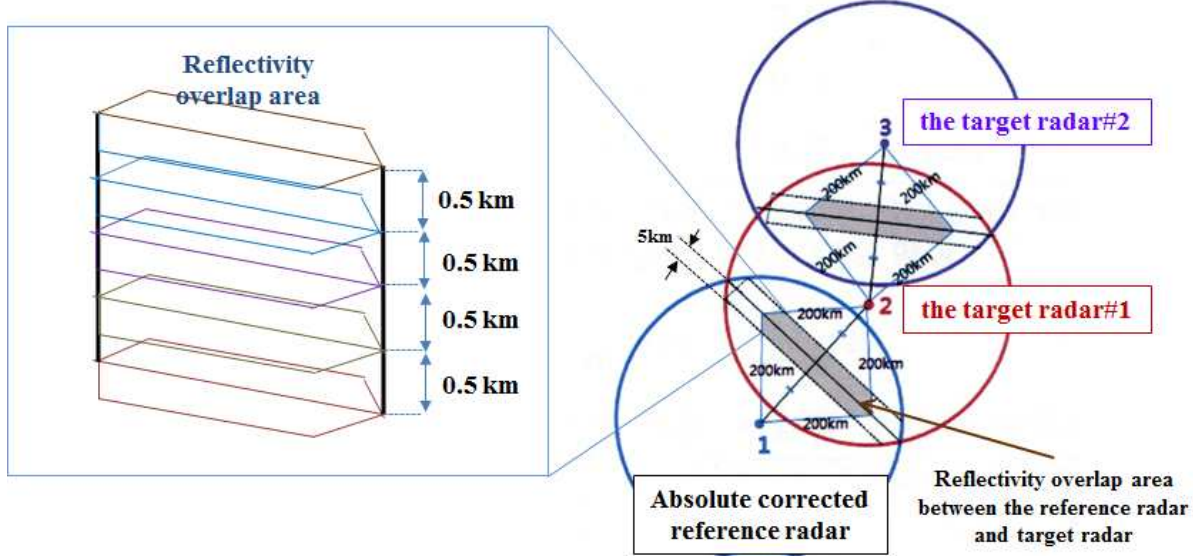
8

9

10

11

12



1

2 **Fig. 4.** The concept of calculating Z-bias for the target radar according to the reference radar
3 reflectivity (Korea Meteorological Administration, 2011)

4

5

6

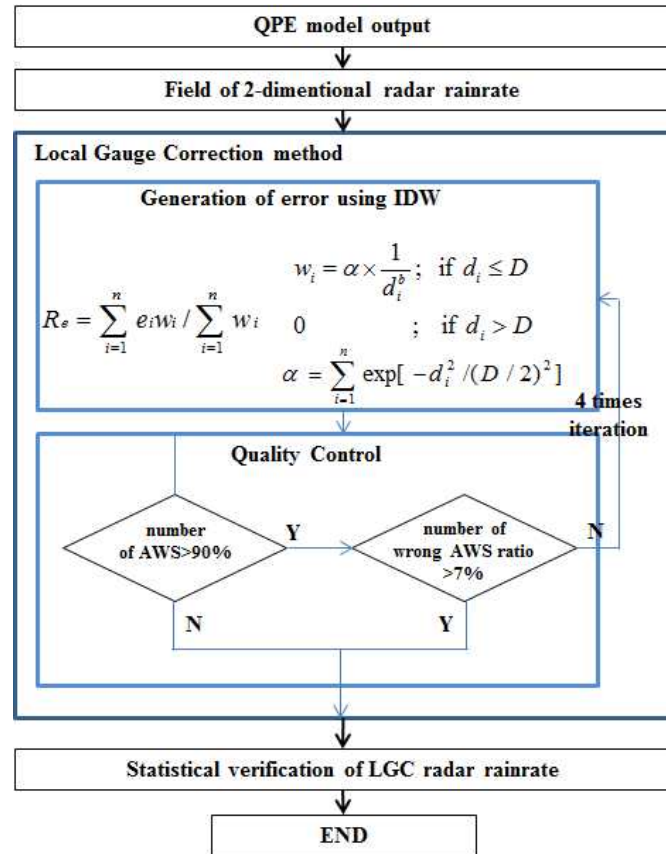
7

8

9

10

11



1

2 **Fig. 5.** Flowchart of the Local Gauge Correction method

3

4

5

6

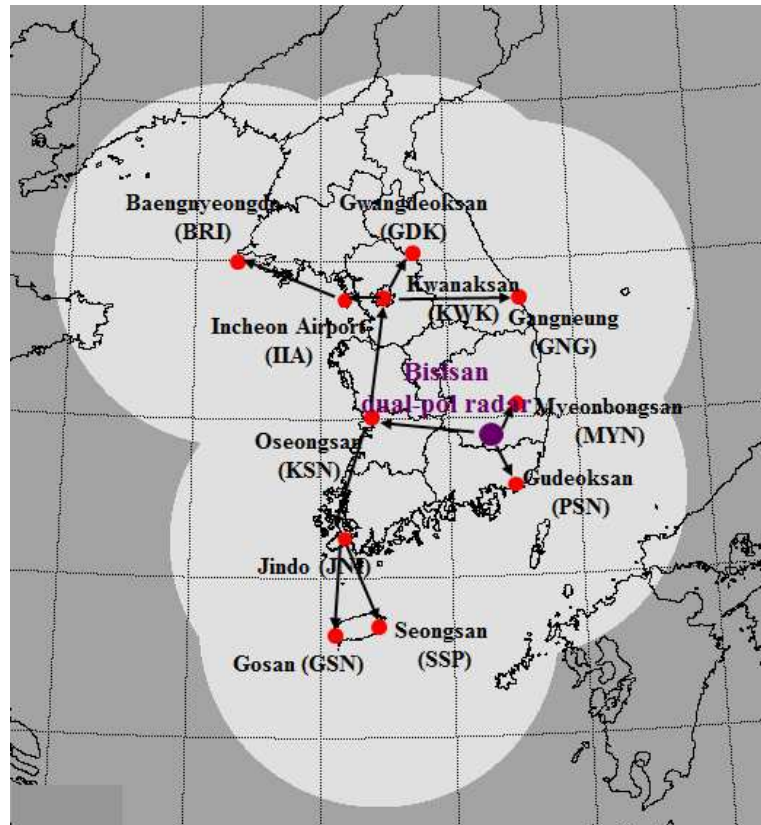
7

8

9

10

11



1

2 **Fig. 6.** Sequence of the reflectivity bias estimation for each radar site

3

4

5

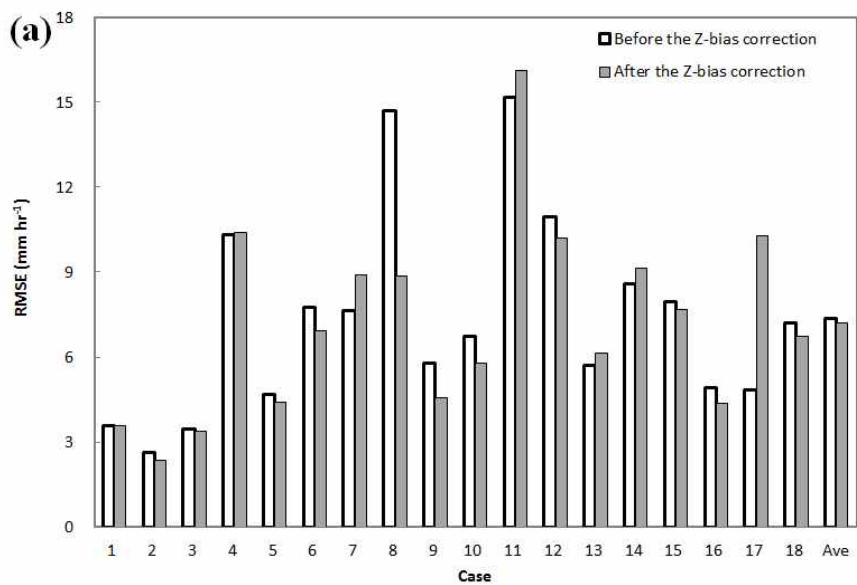
6

7

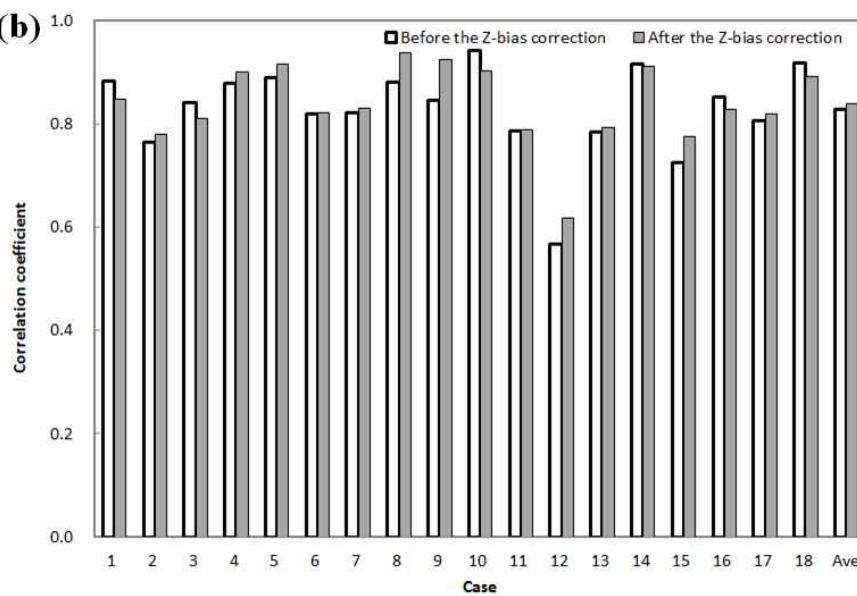
8

9

1



2



3 **Fig. 7.** Comparison of the accuracy of rainfall estimates for each rainfall case before and after
4 the Z-bias correction: (a) RMSE; (b) correlation coefficient

5

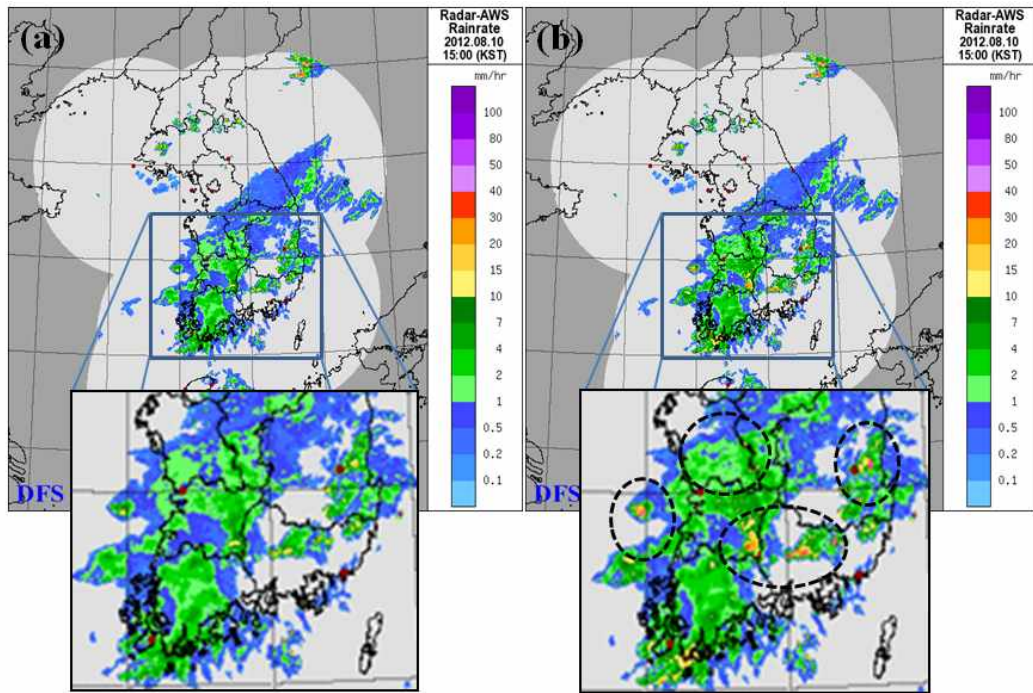
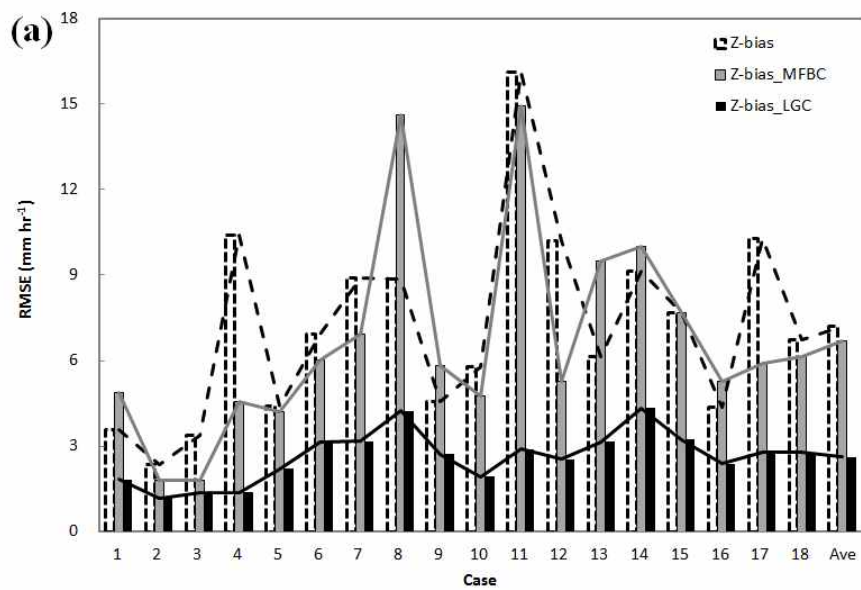


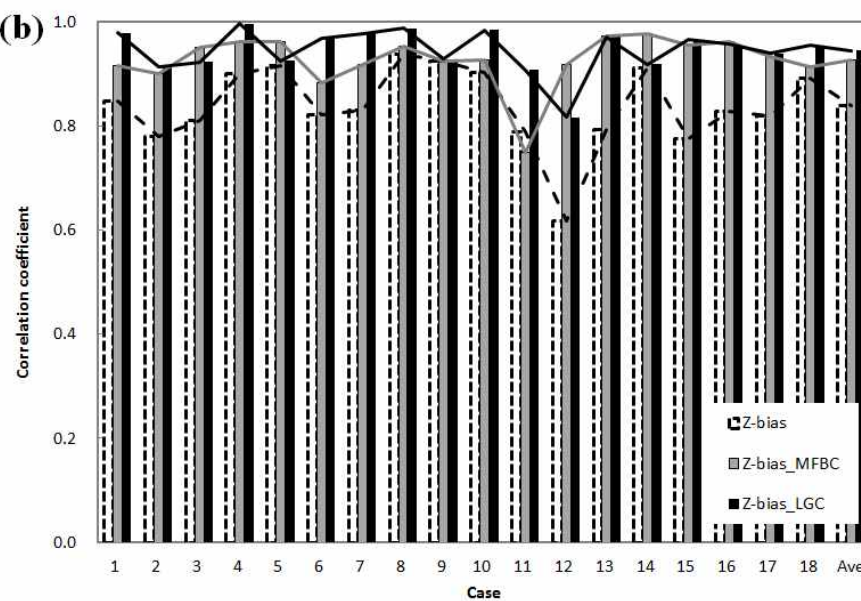
Fig. 8. Comparison of rainfall estimate images in the RAR system before and after the Z-bias correction in Case 12 (at 1500 LST on 10 August in 2012): (a) Before the Z-bias correction; (b) After the Z-bias correction

1
2
3
4
5
6
7
8
9
10
11
12
13
14

1



2



3 **Fig. 9.** Comparison of the rainfall estimation accuracy for each rainfall in the Z-bias, Z-
4 bias_MFBC, and Z-bias_LGC methods: (a) RMSE; (b) correlation coefficient

5

6

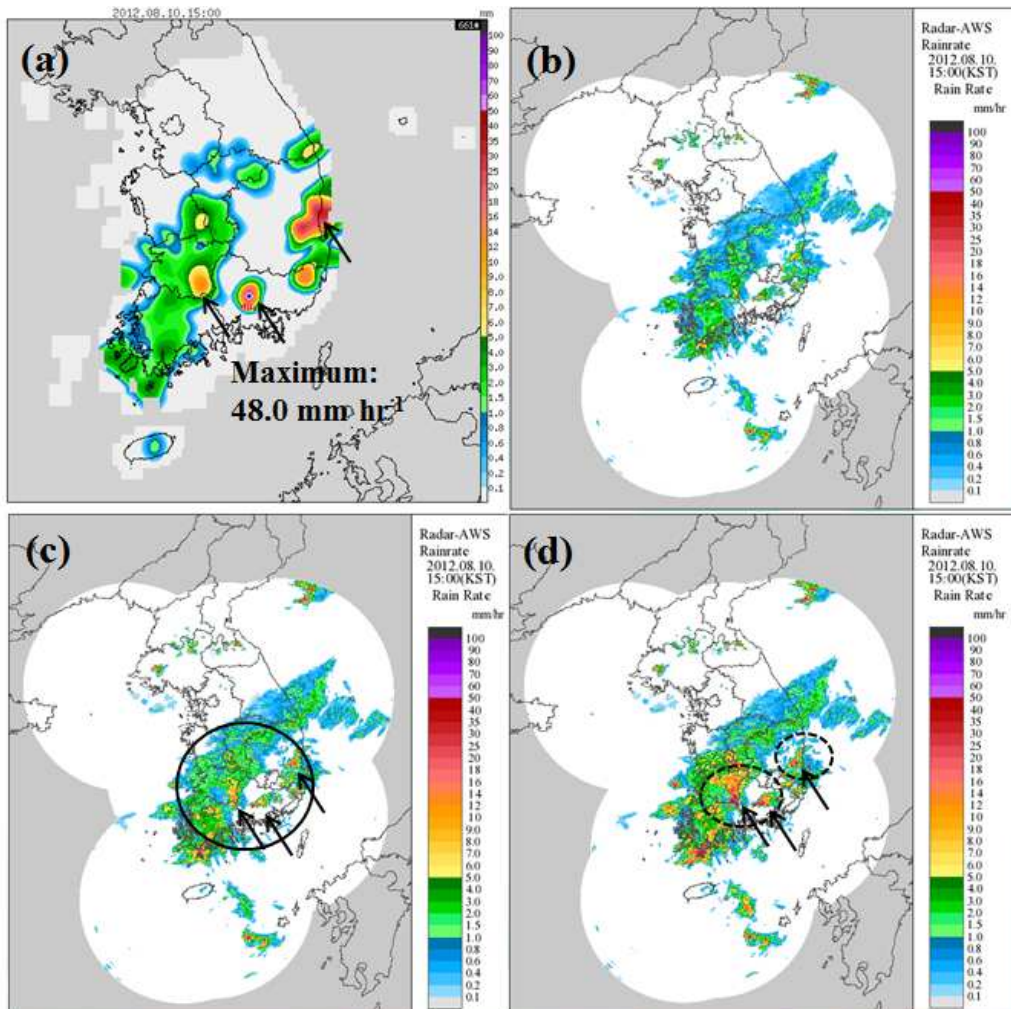
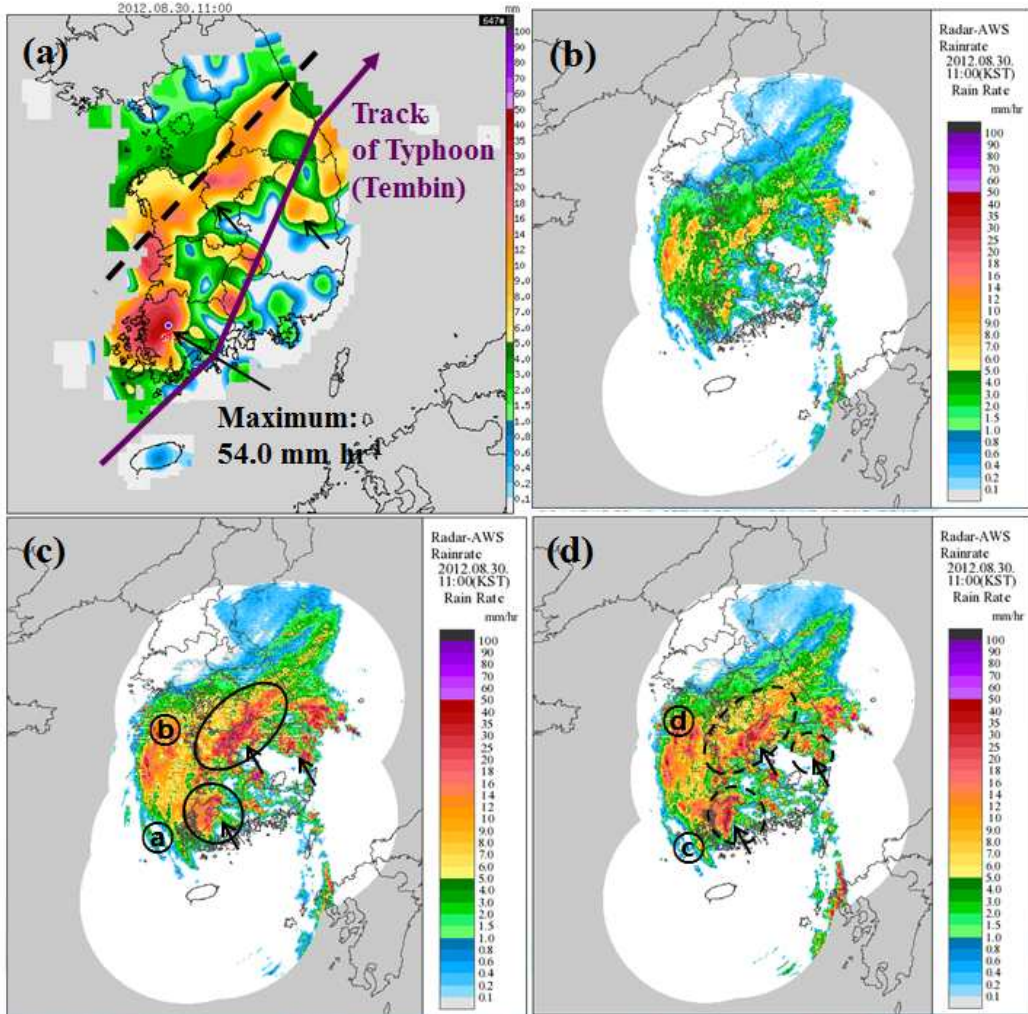


Fig. 10. Comparison of the rainfall images between the AWS and Model Bias Correction method results in Case 12 (at 1500 LST on 10 August in 2012): (a) the AWS; (b) the OBC method; (c) the OBC_MFBC method; (d) the OBC_LGC method

1
2
3
4
5
6
7
8
9
10



1

2 **Fig. 11.** Comparison of the rainfall images between the AWS and Model Bias Correction
 3 method results in Case 18 (at 1100 LST on 30 August in 2012): (a) the AWS; (b) the OBC
 4 method; (c) the OBC_MFBC method; (d) the OBC_LGC method

5

6

7

8

9